Evaluating the Emergent Controls of Stream Water Quality with Similitude and Dimensionless Numbers

Omar I. Abdul-Aziz, Ph.D., A.M.ASCE[1]; and Shakil Ahmed, Ph.D., S.M.ASCE[2]

Abstract: The emergent hydrologic and land-use controls of coastal-urban stream water quality were evaluated by using similitude and dimensional analysis, considering southeast Florida a prototype of growing coastal-urban environments. The goal was to test a fundamental hypothesis that the coastal-urban stream water quality processes represent emergent *ecohydrological-biogeochemical* similitudes (parametric reductions). The in-stream total nitrogen (TN), total phosphorus (TP), and biomass (Chl a) were normalized by their immediate upstream reach concentrations to formulate the dimensionless numbers of TN/TN_0, TP/TP_0, and Chl a/Chl a_0. Stream dissolved oxygen (DO) was normalized by its saturated concentration (DO_{sat}) to obtain the dimensionless DO/DO_{sat} number—avoiding a misleading scaling by upstream concentrations in the presence of a DO sag phenomenon. The emergent controls of stream water quality were represented by a small set of dominant driver dimensionless numbers. For each water quality indicator, nine original variables (including predictors and response) were reduced to three to four important and mechanistically meaningful dimensionless numbers. The *hydrologic control number* (role of watershed hydrology versus the external Everglades) and *salinity number* (ratio of downstream to upstream salinity) exhibited the key controls on stream TN/TN_0 across the wet and dry seasons. In contrast, the *land-use number* (ratio of agricultural plus vegetated lands to built lands), hydrologic control number, and salinity number dominated TP/TP_0 and Chl a/Chl a_0 incorporating the two seasons. However, DO/DO_{sat} was controlled by the *hyporheic exchange number* (role of watershed groundwater versus surface hydrology) and land-use number in the wet and dry seasons, respectively. The formulated similitude and dimensionless numbers provided important insights and understanding that may help achieve healthy coastal-urban streams. **DOI: 10.1061/(ASCE)HE.1943-5584.0001769.** © *2019 American Society of Civil Engineers.*

Author keywords: Coastal-urban streams; Water quality; Environmental controls; Similitude; Dimensional analysis; Florida.

Introduction

Stream water quality and ecosystem health can be shaped by various hydrologic, land-use, biogeochemical, and ecological processes (Caccia and Boyer 2005; Tran et al. 2010; Badruzzaman et al. 2012). The multitude of pollutant sources, drivers, and their interplays pose a major challenge to identify the dominant controls of stream water quality, and understand their contrasting roles as well as collective emergent patterns. The challenge becomes formidable in rapidly expanding coastal-urban environments such as southeast Florida, which represents a low surface elevation, high groundwater table, relatively flat topography, and a complex drainage network. It remains unclear whether the many process drivers of coastal-urban stream water quality can be reduced into a smaller set of composites but simple and interpretable entities. What are the contrasting roles of draining watershed hydrology versus external drivers (from upstream inland and/or downstream coast), watershed surface versus groundwater hydrology, and built-up versus unbuilt (e.g., agriculture, vegetation) land uses in driving stream water quality? What exclusive roles does salinity play in shaping the key indicators of coastal-urban stream water quality? Similitude and dimensional analysis can help answer these questions by incorporating the important physical, chemical, biological, and ecological processes into a small set of dimensionless entities or numbers (Warnaars et al. 2007). Mechanistically meaningful dimensionless numbers can indicate the emerging patterns and provide a generalizable understanding into the dynamics and controls of stream water quality and ecosystem health.

Much research has reported various land uses (urban and nonurban) as the major sources and/or drivers of in-stream nutrients (e.g., nitrogen, phosphorus) and dissolved oxygen in coastal streams (e.g., Tufford et al. 2003; Carey et al. 2011a, b; Wan et al. 2014a, b; Xiao et al. 2016). Among the recent studies, Carey et al. (2011a, b) found watershed agricultural and urban lands contributing large nutrient loads into the inland canals of Biscayne Bay Watershed, Florida. Wan et al. (2014b) reported a strong association of stream water quality with agricultural lands and upstream water management in the Indian River Lagoon Watershed, Florida. Xiao et al. (2016) identified farmland and built-up land as the sources of oxygen demanding materials into the coastal streams of Huzhou City, China. They further reported seasonally varying relationships between the stream water quality and land uses of the draining watersheds. For example, the in-stream chemical oxygen demand and petroleum concentrations were higher during the wet period, whereas the in-stream dissolved total phosphorus and total nitrogen were higher during the dry period.

Alongside land uses, watershed surface hydrologic processes and drivers can influence water quality in coastal as well as noncoastal streams. Kang et al. (2010) found common surface hydrologic features (e.g., size, slope) affecting the land-use contributions to in-stream water quality in Yeongsan Watershed, Korea. Wan et al. (2014a) reported a strong influence of watershed size and

[1]Associate Professor, Dept. of Civil and Environmental Engineering, West Virginia Univ., P.O. BOX 6103, Morgantown, WV 26506-6103 (corresponding author). ORCID: https://orcid.org/0000-0002-3511-6893. Email: oiabdulaziz@mail.wvu.edu

[2]Graduate Research Assistant, Dept. of Civil and Environmental Engineering, West Virginia Univ., P.O. BOX 6103, Morgantown, WV 26506-6103. Email: skahmed@mix.wvu.edu

Note. This manuscript was submitted on May 22, 2018; approved on October 18, 2018; published online on February 26, 2019. Discussion period open until July 26, 2019; separate discussions must be submitted for individual papers. This paper is part of the ***Journal of Hydrologic Engineering***, © ASCE, ISSN 1084-0699.

permeability on the concentration of nutrients in the Xitiaoxi River, China. Tran et al. (2010) found a substantial control of the draining watershed size on the land-use contributions of pollutants into the streams of eastern New York State (upper and lower Hudson Valley, Champlain Valley). Further, Woodcock et al. (2006) reported notable linkages between the distribution of stream biotic communities (e.g., macroinvertebrate taxa) and watershed hydrologic drivers (e.g., water quantity, drainage patterns) in Adirondack Park, New York.

Groundwater has also been found as an important driver of stream water quality. For example, Menció and Mas-Pla (2008) reported that water quality in urbanized Mediterranean streams had been directly linked to the groundwater influxes. Sprague (2005) found groundwater controls on the concentration of dissolved nutrients and calcium bicarbonate in the streams of South Platte River Basin, Colorado. Furthermore, saltwater intrusion is known to impact water quality mainly in coastal streams (Liu et al. 2010). Saltwater intrusion changes the characteristics and composition of aquatic communities (e.g., ammonia-oxidizing bacteria and phytoplankton) and the overall ecosystem (see references in Xie et al. 2017). Magalhães et al. (2005) found a strong, linear decrease of nitrate (NO_3^-) concentrations with increasing salinity in sediments and rocky biofilms of the Douro River estuary, Portugal. Hart et al. (1991) reported adverse effects of high salinity on aquatic plants and invertebrates in the streams, rivers, and wetlands of Australia.

Although the existing literature provides a large body of knowledge and actionable information, there is still a lack of understanding into the contrasting as well as the collective controls of watershed land use, hydrologic, in-stream, and external drivers on stream water quality. In a recent study, Abdul-Aziz and Ahmed (2017) estimated the relative linkages of stream water quality with 11 hydrologic and land-use variables in the coastal-urban watersheds of southeast Florida by using a systematic data analytics framework. However, it is yet to be investigated whether the myriad stream water quality processes and drivers can be combined into a smaller set of emergent and interpretable entities to achieve mechanistically meaningful similitude and useful information. In the field of classical fluid mechanics and hydraulic engineering, similitude is defined as the parametric reduction of physical problems by developing dimensionless numbers and a dimensionless formulation of the physical system (Finnemore and Franzini 2002; Kundu and Cohen 2004). Similitude can be obtained through dimensional analysis (e.g., using Buckingham pi theorem) or through normalizing (i.e., scaling) the underlying governing equations by appropriate characteristic parameters (Kundu and Cohen 2004).

Similitude and dimensional analysis have been used in various science and engineering disciplines to gain insights into the dominant process controls, discover emerging patterns, and formulate parametric reductions (Warnaars et al. 2007; Miragliotta 2011). A classic example of similitude in hydraulic engineering can be the Moody diagram for pipe flow design (Finnemore and Franzini 2002). Dimensional analysis reduced seven original parameters for pipe flow (flow velocity, pressure, viscosity, density, pipe diameter, length, and roughness) to three mechanistically meaningful dimensionless numbers (pipe friction factor, Reynolds number, and relative roughness). Warnaars et al. (2007) applied similitude and dimensional analysis in stream biogeochemistry and ecology, and estimated scaling relationships of biotic variable (e.g., biomass) with abiotic (e.g., climatic, hydrologic, and geomorphic) variables in different streams across North America. Other recent studies (e.g., Morris and Hondzo 2013; Zeleňáková et al. 2013; Guentzel et al. 2014) used similitude and dimensional analysis to investigate and predict the dynamics of stream water quality indicators (e.g., nitrogen, phosphorus, and dissolved oxygen) in various hydraulic, hydrologic, and ecological conditions.

The goal of this study is to test a fundamental hypothesis that the coastal-urban stream water quality processes represent emergent *ecohydrological-biogeochemical* similitudes (parametric reductions). In this pursuit, southeast Florida was considered as a prototype of growing coastal-urban environments to achieve two specific research objectives. First, similitude and dimensional analysis are used to formulate mechanistically meaningful dimensionless numbers, and the dominant dimensionless numbers are identified by using a systematic data analytics methodology. Second, the emergent (contrasting as well as collective) controls of water quality in the coastal-urban streams are evaluated by interpreting the dimensionless numbers. The research findings are expected to guide water resources management to achieve and/or maintain healthy stream ecosystems in complex coastal-urban environments.

Materials and Methods

Study Area

The study area is located between the Biscayne Bay and the Indian River Lagoon Watersheds of southeast Florida, representing Broward County and a part of Palm Beach County (Fig. 1). The region is primarily drained by a large network of natural and dredged canals (Broward County 2016), including five major canal basins as follows: Hillsboro Canal, C-14 Canal (Cypress Creek, Pompano Canal), C-13 Canal, North New River (NNR) Canal, and C-11 Canal. The canals are connected to the Florida Everglades water

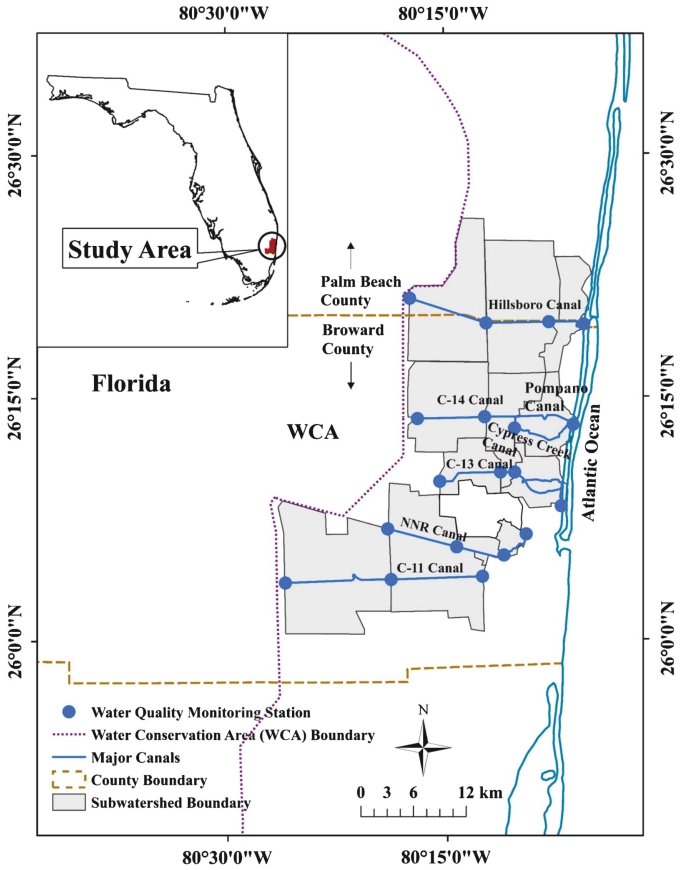

Fig. 1. Locations of water quality monitoring stations in major canals and corresponding watershed boundaries. Inset shows state of Florida.

Table 1. Summary of the stream water quality indicators and their drivers during 2009–2013

Variables	Mean	Standard deviation	Minimum	25th percentile	50th percentile	75th percentile	Maximum
L_c (km)	12.26	4.20	6.71	9.17	12.10	15.04	21.31
D_c (km)	9.86	5.57	1.40	5.27	10.28	13.77	21.01
A_{AGR} (km^2)	5.61	9.42	0.06	0.31	1.37	7.07	29.37
A_{BUL} (km^2)	36.32	23.31	4.88	19.84	29.98	54.97	79.77
			Wet season (June–October)				
TN (mg/L)	1.33	0.28	0.75	1.25	1.41	1.48	1.77
TP (mg/L)	0.04	0.03	0.02	0.02	0.03	0.05	0.11
Chl *a* (μg/L)	7.03	2.93	3.39	5.12	6.46	8.61	15.94
DO (mg/L)	4.02	0.96	1.61	3.24	4.50	4.77	5.21
DO_{sat} (mg/L)	7.51	0.31	7.02	7.16	7.63	7.73	7.92
Sal (ppt)	3.07	5.93	0.13	0.18	0.28	1.58	19.40
GWD (10^{-3} km)	1.96	0.74	0.79	1.38	1.84	2.63	3.11
			Dry season (November–May)				
TN (mg/L)	1.23	0.34	0.57	0.95	1.29	1.49	1.63
TP (mg/L)	0.04	0.02	0.02	0.02	0.03	0.05	0.09
Chl *a* (μg/L)	4.76	2.26	2.13	2.73	4.19	6.18	10.37
DO (mg/L)	5.81	0.99	3.34	5.72	6.13	6.28	7.10
DO_{sat} (mg/L)	8.13	0.54	7.34	7.51	8.47	8.56	8.72
Sal (ppt)	5.64	9.14	0.03	0.04	0.08	14.98	24.13
GWD (10^{-3} km)	2.11	0.78	0.77	1.53	1.99	2.86	3.42

Note: L_c, D_c, GWD, A_{AGR}, and A_{BUL}, respectively, refer to subbasin characteristic length, distance of subbasin outlet from the coastline, groundwater depth from land surface, agricultural plus vegetated land area, and built-up land area.

conservation areas (WCAs) at the west (upstream) and to the Atlantic Ocean at the east (downstream) (Fig. 1). The in-stream biogeochemistry and water quality are influenced by the WCAs and coastal hydrology (BCEPD 2007). Together, the canals represent a considerable physical, biogeochemical, and ecological range of coastal-urban watersheds (Table 1), draining approximately 865 km^2 of highly urban areas to the Atlantic Ocean. More details on the canals can be found in Cooper and Lane (1987) and BCEPD (2007).

Data Sets

The water quality data set represented quarterly time-series data of commonly-used indicators such as total nitrogen (TN), total phosphorus (TP), chlorophyll *a* (Chl *a*), dissolved oxygen (DO), and salinity (Sal) during 2009–2013 for 19 monitoring stations across the study area (Fig. 1). The data were collected and made available to the public by Broward County Environmental Planning and Community Resilience Division (BCEPCRD 2015). The four water quality indicators can provide information on the general health of a stream ecosystem (Chang 2008; Daniel et al. 2010; Wan et al. 2014a). TN represented an aggregation of total Kjeldahl nitrogen (TKN), nitrate-nitrogen (NO_3-N), and nitrite-nitrogen (NO_2-N). TP included orthophosphates (reactive phosphates), condensed phosphates (pyro, meta, and polyphosphates), and organic phosphates. Chl *a* indicated oxygenic photosynthesis by the stream flora (mainly phytoplankton). DO represented a more holistic indicator of stream water quality and ecosystem health. Details into the water quality data collection methods, protocols, and QA/QC can be found in BCEPD (2007) and FDEP (2016).

We delineated drainage areas (subbasins) for the 14 downstream monitoring stations (i.e., 19 minus the five most upstream stations) from 10-m DEM (USGS 2015a) by using ESRI ArcGIS version 10.2. The derived subbasin areas were verified and corrected (if needed) by comparing with the well-established waterbody identification numbers (FDEP 2016) and a contribution area map provided by Broward County (Robert Bernhard, personal communications, 2012). Subbasin characteristic length (L_c; defined as the longest flow path to the subbasin outlet) was computed to represent the watershed surface hydrologic controls on the in-stream water quality. The groundwater hydrologic control was represented by the groundwater depth (GWD) from the land surface, which decreases as the water table moves upward. Groundwater level data from 29 monitoring stations of (USGS 2015b) were used with kriging interpolations (Goovaerts 1997; Childs 2004; Costelloe et al. 2015) to determine the ambient GWD for each in-stream water quality station.

The canal centerline distance of each subbasin outlet (water quality station) from the coastline (D_c)—which decreases toward the coast and increases toward the Everglades—was computed to represent the effects of both tidal and Everglades hydrology on stream water quality. The coastal control on the in-stream water quality was further represented by the concentration of salinity at the inlet and outlet (Sal_0 and Sal, respectively; *0* indicates the immediate upstream station) of each stream reach. Abdul-Aziz and Ahmed (2017), in a separate study, reported built-up, agricultural, and vegetated areas as the most dominant land uses impacting the urban stream water quality in southeast Florida. The controls of land uses were therefore represented by the built (A_{BUL}) and nonurban (i.e., unbuilt) areas (A_{AGR} = agriculture + vegetation). Land-use information was collected from the land use and land cover (LULC) database of the SFWMD (2015a), and processed in ESRI ArcGIS version 10.2.

Acknowledging the seasonal variation of climate and hydrology, we performed separate, comparative analyses for the wet (June–October) and dry (November–May) seasons (SFWMD 2015b). For each season, the spatial data set was obtained by averaging observations of the respective water quality and groundwater data over the five-year period (2009–2013). The saturated concentrations of DO (DO_{sat}) at each water quality station were estimated as a nonlinear function of water temperature, salinity, and atmospheric pressure (Chapra 2008). Water temperature data for the stations were collected from the National Water Quality Monitoring Council (NWQMC) database (NWQMC 2017). However, three water quality stations did not have water temperature data, which were estimated from air temperature through a linear regression between air and water temperatures for the nearest water quality station that had observed data for both temperatures (r^2 = 0.78–0.89, p-value < 0.05). The air temperature data were obtained from the

NSRDB (2017). Atmospheric pressure data were collected from the DBHYDRO database of the South Florida Water Management District (SFWMD 2016).

The final data set incorporated concentrations of water quality variables (TN, TP, Chl *a*, DO, DO_{sat}, and Sal) at the inlets and outlets of 14 reaches, as well as areas of important land uses (A_{AGR} and A_{BUL}) and hydrologic features (L_c, D_c, and GWD) for the corresponding subbasins. Sample size of the temporally averaged spatial data set for each water quality variable was 14. TN, TP, Chl *a*, and DO were considered the response water quality indicators, whereas Sal was treated as an oceanic biogeochemical driver of the response variables. The water quality variables, as well as their hydrologic and land-use drivers had considerable variation and ranges across the entire study area (Table 1) and within each of the five major canal basins (Table S1 in Supplemental Data).

Dimensional Analysis, Similitude, and Formulation of Dimensionless Numbers

We used dimensional analysis to achieve similitude and derive dimensionless numbers by using the Buckingham pi theorem (Finnemore and Franzini 2002; Kundu and Cohen 2002). The pi theorem states that *n* dimensional variables can be combined to form (n-r) dimensionless Π numbers, in which r is the number of involved fundamental dimensions. The method is based on the principle of dimensional homogeneity, requiring the incorporation of mechanistically relevant variables. The important process variables for the four water quality indicators (TN, TP, Chl *a*, DO) were identified based on existing knowledge (e.g., Abdul-Aziz and Ahmed 2017) and a preliminary analysis of data sets (e.g., scatter plot of a possible driver versus response). For example, TN at a monitoring site is considered to be a response function of concentrations at the immediate upstream station (TN_0), at-site and immediate upstream salinity (Sal and Sal_0), external influence from the bay and/or the Everglades (D_c), and draining subbasin's hydrologic and land-use features (L_c, GWD, A_{AGR}, and A_{BUL}). A first expression of the functional form can be stated as follows:

$$f(TN, TN_0, Sal, Sal_0, L_c, D_c, GWD, A_{AGR}, A_{BUL}) = 0 \quad (1)$$

The total number of variables, n = 9; number of relevant fundamental dimensions, r = 2 (mass: M; length: L) (see Table 2 for dimensions of all variables); and the total possible dimensionless (Π) numbers = n − r = 7. Thus, Eq. (1) can be rewritten in terms of pi numbers as follows:

$$\phi(\Pi_1, \Pi_2, \Pi_3, \Pi_4, \Pi_5, \Pi_6, \Pi_7) = 0 \quad (2)$$

The pi theorem led to the selection of two (r = 2) *repeating variables*, which must contain all the involved fundamental dimensions (M and L for this study) and must not form a dimensionless number by themselves. Each pi number was formulated by combining two repeating variables with one of the remaining variables. For example, considering TN_0 and L_c as the repeating variables, the first pi number was formulated with the exponents of *a* and *b* as follows:

$$\Pi_1 = TN_0{}^a L_c^b D_c \quad (3)$$

For Π_1 to be dimensionless, the following equation was obtained using the principle of dimensional homogeneity:

$$M^0L^0 = \left(\frac{M}{L^3}\right)^a (L)^b (L) = M^a L^{-3a+b+1} \quad (4)$$

Equating the exponents on both sides, we found the following: a = 0, b = −1; therefore

$$\Pi_1 = (TN_0)^0 (L_c)^{-1} (D_c) = \left(\frac{D_c}{L_c}\right) \quad (5)$$

Similarly, the other pi numbers (Π_2 to Π_7) were formulated as follows:

$$\Pi_2 = \frac{GWD}{L_c}; \quad \Pi_3 = \frac{TN}{TN_0}; \quad \Pi_4 = \frac{A_{AGR}}{L_c^2};$$
$$\Pi_5 = \frac{A_{BUL}}{L_c^2}; \quad \Pi_6 = \frac{TN_0}{Sal}; \quad \Pi_7 = \frac{TN_0}{Sal_0}$$

Based on the pi theorem, the functional relationship between the response (TN/TN_0) and predictor pi numbers can be expressed as follows:

$$\frac{TN}{TN_0} = \phi\left[\left(\frac{D_c}{L_c}\right)\left(\frac{GWD}{L_c}\right)\left(\frac{A_{AGR}}{L_c^2}\right)\left(\frac{A_{BUL}}{L_c^2}\right)\left(\frac{TN_0}{Sal}\right)\left(\frac{TN_0}{Sal_0}\right)\right] \quad (6)$$

The pi theorem allows combining relevant pi numbers to derive a new pi number (e.g., A_{AGR}/L_c^2 and A_{BUL}/L_c^2 to A_{AGR}/A_{BUL}; TN_0/Sal and TN_0/Sal_0 to Sal/Sal_0). It also allows inversing any pi number based on convenience for interpretations (e.g., D_c/L_c to L_c/D_c). Various sets of pi numbers were derived by changing the repeating variables for TN, TP, Chl *a*, and DO (see Appendix S1); only the mechanistically meaningful sets of pi numbers were retained for further analysis. Following numerous diligent iterations, we obtained meaningful sets of five pi numbers for each water quality indicator. The analysis therefore led to a meaningful set of four response and four predictor pi numbers, which can be expressed in functional forms as follows:

$$\frac{TN}{TN_0} = \phi\left[\left(\frac{L_c}{D_c}\right)\left(\frac{GWD}{L_c}\right)\left(\frac{A_{AGR}}{A_{BUL}}\right)\left(\frac{Sal}{Sal_0}\right)\right] \quad (7)$$

$$\frac{TP}{TP_0} = \phi\left[\left(\frac{L_c}{D_c}\right)\left(\frac{GWD}{L_c}\right)\left(\frac{A_{AGR}}{A_{BUL}}\right)\left(\frac{Sal}{Sal_0}\right)\right] \quad (8)$$

$$\frac{Chla}{Chla_0} = \phi\left[\left(\frac{L_c}{D_c}\right)\left(\frac{GWD}{L_c}\right)\left(\frac{A_{AGR}}{A_{BUL}}\right)\left(\frac{Sal}{Sal_0}\right)\right] \quad (9)$$

$$\frac{DO}{DO_{sat}} = \phi\left[\left(\frac{L_c}{D_c}\right)\left(\frac{GWD}{L_c}\right)\left(\frac{A_{AGR}}{A_{BUL}}\right)\left(\frac{Sal}{Sal_0}\right)\right] \quad (10)$$

Table 2. List of the variables used in similitude analyses and their dimensions

Variables	Dimensions
Concentration of water quality indicators and salinity at watershed outlet (TN, TP, Chl *a*, DO, Sal)	(M/L^3)
Concentration of water quality indicators and salinity at watershed inlet (TN_0, TP_0, Chl a_0, Sal_0)	(M/L^3)
Saturated concentration of dissolved oxygen (DO_{sat})	(M/L^3)
Characteristic length of subbasin (L_c)	(L)
Distance from the coastline (D_c)	(L)
Groundwater depth from land surface (GWD)	(L)
Agricultural and vegetated land (A_{AGR})	(L^2)
Built-up land (A_{BUL})	(L^2)

Response pi numbers such as the *total nitrogen number* (TN/TN_0), *total phosphorus number* (TP/TP_0), and *biomass number* ($Chl\,a/Chl\,a_0$) represented, respectively, the outlet concentrations of TN, TP, and Chl *a* for each subbasin, as normalized by their inlet concentrations (TN_0, TP_0, and $Chl\,a_0$). However, the stream *dissolved oxygen number* (DO/DO_{sat}) represented the outlet concentrations of DO normalized by the corresponding oxygen dissolution capacity of stream water (i.e., DO at saturation, DO_{sat}). This normalization helped avoid a misleading scaling of DO by the corresponding upstream reach concentration (i.e., DO_0), which may be impacted by the well-known DO sag phenomenon in streams (Chapra 2008). The four predictor pi numbers represented the pairwise collective controls of various environmental drivers on the urban stream water quality processes. L_c/D_c represented the control of watershed hydrology on stream water quality relative to the external Everglades (upstream) and/or ocean (downstream), and was termed the hydrologic control number. GWD/L_c represented the control of groundwater hydrology relative to the watershed surface hydrology, and was termed the hyporheic exchange number. The land-use number (A_{AGR}/A_{BUL}) represented the control of nonurban (agriculture and vegetation) land relative to the built-up land. The salinity number (Sal/Sal_0) represented the control of at-site salinity (normalized by salinity at the immediate upstream reach) on the water quality. Data summary of the response and predictor pi numbers indicated a considerable range among the 14 stream reaches (Table 3) and across the five canal basins (see Table S2 in Supplemental Data). Although all pi numbers varied between the wet and dry seasons, Sal/Sal_0 was strikingly higher (10 times in both mean and standard deviation) in the dry season (Table 3)—indicating high salt water intrusion in the downstream stations during low freshwater flows in the canals.

Overall for each of the water quality response variables (TN, TP, Chl *a*, DO), dimensional analysis reduced nine original variables to a set of five meaningful pi numbers. Recalling the definition of similitude from fluid mechanics and hydraulic engineering (Finnemore and Franzini 2002; Kundu and Cohen 2002), such a parametric reduction of stream water quality processes was termed stream ecohydrological-biogeochemical similitude in this research. The parametric reduction is particularly useful for small data sets, which is often the case for stream water quality and ecosystem health problems. For example, the sample size for each water quality indicator here was 14, which provided ample degrees of freedom to estimate a water quality number as a function of four predictor pi numbers (a total of five dimensionless numbers). The relationships between the response (Π_1) and predictor pi (Π_2-Π_5) numbers [Eqs. (7)–(10)] can be represented as a general power-law model as follows:

$$\Pi_1 = k\Pi_2^c\Pi_3^d\Pi_4^e\Pi_5^g \tag{11}$$

where the coefficient (k) and exponents (c, d, e, g) have to be estimated by fitting with observational data for the involved pi numbers. However, upon data standardization and resolution of any multicollinearity among the pi numbers (see the following section for details), the model estimation process would indicate the relative contribution of each predictor pi number to the explanation of variance in a response pi number. This could identify a smaller set of effective and dominant predictor pi numbers for each water quality response pi number—contributing further into the parametric reductions and stream ecohydrological-biogeochemical similitude.

Identification of the Dominant Dimensionless Numbers

We used a systematic data analytics methodology (Abdul-Aziz and Ahmed 2017) to identify the dominant, mechanistically meaningful predictor pi numbers for each water quality response pi number. The data analytics involved a sequential application of four complementary data-mining tools: Pearson correlation matrix, principal component analysis (PCA), factor analysis (FA), and partial least squares regression (PLSR). Convergent information from different tools was synthesized to arrive at the overall outcomes. The data analytics were performed with logarithmically transformed and standardized (Z-score) data of each pi number as follows: $Z = (X - \bar{X})/s_X$, where $X = \log_{10}$-transformed data of a pi number, $\bar{X}$ = mean of X, and s_X = standard deviation of X. The log-transformation accounted for any nonlinear interactions in the data system, whereas the Z-scores brought different pi numbers to a comparable reference scale. The entire analyses and modeling were performed by using MATLAB version R2016a.

Pearson correlation matrix with Z-scores of log-transformed pi numbers provided first-order information on the nonlinear correspondences between predictor versus response pi numbers, and among the predictor pi numbers (i.e., multicollinearity on the $\log_{10}$ space). PCA (Jolliffe 2002) resolved multicollinearity by deriving eight orthogonal entities called principal components (PCs); each

Table 3. Overall summary of the dimensionless numbers across all sites during 2009–2013

Dimensionless numbers	Mean	Standard deviation	Minimum	25th percentile	50th percentile	75th percentile	Maximum
L_c/D_c	2.08	2.03	0.56	0.79	1.15	2.90	6.91
A_{AGR}/A_{BUL}	0.12	0.16	0.002	0.02	0.05	0.12	0.50
			Wet season (June–October)				
TN/TN_0	0.88	0.15	0.63	0.82	0.91	0.96	1.24
TP/TP_0	1.52	0.83	0.94	0.98	1.36	1.59	4.23
$Chl\,a/Chl\,a_0$	1.05	0.47	0.56	0.64	0.89	1.51	1.85
DO/DO_{sat}	0.58	0.11	0.35	0.49	0.61	0.63	0.74
Sal/Sal_0	13.20	26.24	0.53	0.91	2.09	9.84	89.60
GWD/L_c (10^{-4})	1.81	0.95	0.37	1.22	1.42	2.50	3.81
			Dry season (November–May)				
TN/TN_0	0.82	0.17	0.49	0.68	0.88	0.93	1.09
TP/TP_0	1.50	0.61	0.93	1.06	1.27	1.85	3.09
$Chl\,a/Chl\,a_0$	1.28	0.76	0.34	0.83	1.01	1.46	2.83
DO/DO_{sat}	0.75	0.10	0.53	0.68	0.79	0.83	0.84
Sal/Sal_0	121.11	245.15	0.47	0.78	1.36	111.01	739.46
GWD/L_c (10^{-4})	1.96	1.04	0.36	1.32	1.60	2.67	4.19

Note: TN/TN_0, TP/TP_0, $Chl\,a/Chl\,a_0$, and Sal/Sal_0, respectively, are the normalized concentrations of TN, TP, Chl *a*, and Sal by their respective inlet concentrations. DO/DO_{sat} is the normalized concentration of DO by its saturation concentration.

PC was as a linear combination of all eight (four response and four predictor) pi numbers. However, FA (Jolliffe 2002) resolved multicollinearity by decomposing all pi numbers into a smaller set of orthogonal, latent entities called factors. Loadings of pi numbers on each factor were optimized by performing a *varimax* rotation. The eigenvalue ≥ 1 criterion was used to extract an optimal number of factors that described the most data-system variance. Given the reverse but complementary methodologies, PCA and FA were used in concert to achieve an unbiased and confirmatory representation of interrelations among the predictor as well as response pi numbers.

Finally, PLSR modeling (Wold et al. 2001) was used to directly estimate the relative linkages between each response and the four predictor pi numbers through a simultaneous decomposition of the targeted response and all predictors (Schumann et al. 2013). Each response pi number was fitted separately on the transformed orthogonal domain with a minimum number of independent partial least squares (PLS) components, which were linear combinations of only the predictor pi numbers. The PLSR models were optimized using a synthesis of the minimum Akaike information criteria (AIC) (Akaike 1974) and the maximum Nash-Sutcliffe efficiency (NSE) criteria (Nash and Sutcliffe 1970) to resolve any bias and instability caused by multicollinearity among the predictor pi numbers. The optimal PLSR models were estimated by using SIMPLS algorithm (de Jong 1993; Hubert and Branden 2003) and a 10-fold cross validation method (Kuhn and Johnson 2013). The estimated model coefficients associated with the optimal PLS components were then transformed back from the orthogonal domain to the Z-score domain of $\log_{10}$-transformed pi numbers. The transformed PLSR model coefficients represented the estimated relative linkages (β) of a response pi number with the predictor numbers. The efficiency and accuracy of the final PLSR models of Z-scores were, respectively, measured by NSE and the ratio of root-mean-square error to the standard deviation of the observations (RSR).

Results

Mutual Correspondences of the Dimensionless Numbers

The nonlinear correspondences between the response and predictor pi numbers ($\log_{10}$-transformed and standardized) were first examined by computing correlation coefficients (r) for wet and dry seasons separately (Table 4). Across the two seasons, the in-stream *total nitrogen number* (TN/TN_0) had strong correlations with the *hydrologic control number* (L_c/D_c; $r = -0.62$ to -0.75) and with the salinity number (Sal/Sal_0; $r = -0.78$ to -0.87). However, the *total phosphorus number* (TP/TP_0) had moderate to strong correlations with only the land-use number (A_{AGR}/A_{BUL}; $r = 0.49$ to 0.62) in the two seasons. The stream biomass number ($Chl\,a/Chl\,a_0$) also showed a moderate to strong correlation with A_{AGR}/A_{BUL} ($r = 0.57$) in the wet season; however, $Chl\,a/Chl\,a_0$ was relatively strongly correlated with L_c/D_c in both seasons ($r = -0.60$ to -0.66). The stream dissolved oxygen number (DO/DO_{sat}) had strong correlations with the hyporheic exchange number (GWD/L_c; $r = 0.70$) and A_{AGR}/A_{BUL} ($r = -0.74$) in the wet and dry seasons, respectively. Further, moderate correlations of DO/DO_{sat} were found with L_c/D_c ($r = 0.48$) and Sal/Sal_0 ($r = 0.55$) in the wet season, and with GWD/L_c ($r = 0.57$) in the dry season.

The correlation matrices (Tables S3 and S4 in Supplemental Data) further represented the mutual correspondences among all pi numbers, suggesting a considerable multicollinearity in the data matrices and meriting orthogonal analysis such as PCA, FA, and PLSR. For example, a strong correlation ($r = 0.74$) was found between Sal/Sal_0 and L_c/D_c in the wet season—indicating the increasing salinity (i.e., increasing Sal/Sal_0) with the decreasing D_c (increasing L_c/D_c) toward the coast (verified by scatter-plots). However, Sal/Sal_0 had a much-reduced correlation with L_c/D_c in the dry season ($r = 0.47$), indicating the effectiveness and frequent operation of salinity control structures to reduce saltwater intrusion during low freshwater flows in the canals (Xie et al. 2017). Further, a moderate correlation ($r = -0.55$ to -0.57) was found between A_{AGR}/A_{BUL} and GWD/L_c across the two seasons. Given GWD increases downward, the negative correlations indicated the beneficial effects of agricultural/vegetated land and adverse impacts of built land on the groundwater-surface water interactions by, respectively, elevating and lowering the water table through basin infiltration and aquifer recharge processes. Among the water quality indicator numbers, $Chl\,a/Chl\,a_0$ had a strong correlation with TP/TP_0 across the wet and dry seasons ($r = 0.61$ to 0.68), indicating TP as the limiting nutrient. Further, the moderate/strong correlations of TN/TN_0 with $Chl\,a/Chl\,a_0$ ($r = 0.60$) and with DO/DO_{sat} ($r = -0.56$) in the wet season indicated the role of TN to drive a potential eutrophication in the canals.

Table 4. Pearson correlation coefficients (r) between the response and predictor pi numbers

Response pi numbers	Season	Predictor pi numbers			
		L_c/D_c	GWD/L_c	A_{AGR}/A_{BUL}	Sal/Sal_0
TN/TN_0	Wet	**−0.75**	−0.11	0.16	**−0.78**
	Dry	**−0.62**	−0.34	0.16	**−0.87**
TP/TP_0	Wet	−0.18	−0.03	**0.62**	−0.10
	Dry	−0.23	0.00	0.49	0.28
$Chl\,a/Chl\,a_0$	Wet	**−0.66**	−0.06	**0.57**	−0.37
	Dry	**−0.60**	0.01	0.29	0.22
DO/DO_{sat}	Wet	0.48	**0.70**	−0.40	**0.55**
	Dry	0.11	**0.57**	**−0.74**	0.40

Note: Data for all pi numbers were $\log_{10}$ transformed to incorporate any nonlinear correspondences. Correlations in bold are significant at the 95% level of confidence from a two-tailed test.

Relative Orientations and Groupings of the Dimensionless Numbers

Among the eight PCs for eight pi numbers representing all involved water quality response and predictor variables, the first two PCs explained approximately 65%–71% of the total data variance across the two seasons (see Table S5 in Supplemental Data). The nonlinear loadings of the pi numbers on the first two PCs were therefore represented through biplots [Figs. 2(a and b)].

Three groups were apparent on the PCA biplots for both wet and dry seasons: (1) A_{AGR}/A_{BUL}, TP/TP_0, and $Chl\,a/Chl\,a_0$; (2) L_c/D_c and Sal/Sal_0; and (3) GWD/L_c and DO/DO_{sat}. Based on the relative orientations and length of vectors, Group 1 variables appeared to be strongly linked with each other—reemphasizing the dominant role of the subbasin's unbuilt (e.g., agriculture and vegetation) versus built land to drive stream TP (limiting nutrient) and biomass in the corresponding stream reach. The positive linkages of Group 2 variables, as well as their strong negative linkages with TN/TN_0, indicated the detrimental impacts of increasing Sal/Sal_0 (increasing salinity) on stream nitrogen with an increasing L_c/D_c (decreasing D_c) toward the coast. The nearly orthogonal orientation of TN/TN_0 with A_{AGR}/A_{BUL} suggested that subbasin

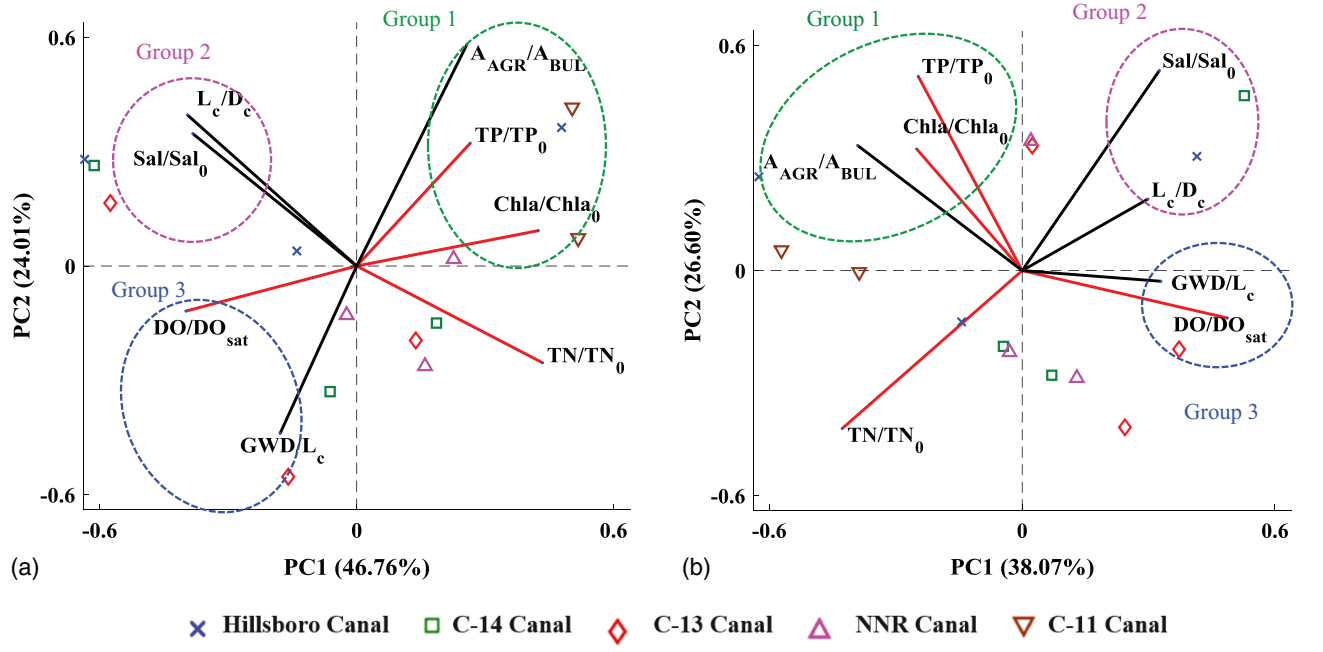

Fig. 2. Biplots from principal component analysis showing interrelation patterns of predictor pi numbers and response pi numbers in (a) wet season (June–October); and (b) dry season (November–May). Percent variance explained by each PC is shown in parenthesis.

land uses had not been any major sources of TN in these urban streams. Instead, increasing TN/TN_0 with the decreasing L_c/D_c (increasing D_c) toward the upstream watersheds indicated the Everglades as the primary source of in-stream nitrogen. Further, the orientation of TN/TN_0 and Chl a/Chl a_0 vectors suggested their strong positive linkage in the wet season and weak linkage (nearly orthogonal) in the dry season. Group 3 represented a strong positive linkage between GWD/L_c and DO/DO_{sat}, indicating the dominant effect of groundwater inputs over the surface flow length and pollutant runoff on stream DO across both seasons. Relative orientations and opposite directions of vectors also indicated the negative impacts of higher A_{AGR}/A_{BUL}, TP/TP_0, Chl a/Chl a_0, and TN/TN_0 on DO/DO_{sat}, as well as that of increasing A_{AGR}/A_{BUL} on GWD/L_c. Further, the orientations of Group 2 variables with DO/DO_{sat} suggested its notable positive linkages with L_c/D_c and Sal/Sal_0.

Based on the closeness to the tip of the corresponding vectors, the PC scores on the biplots demonstrated a good distribution of the response and predictor pi numbers with relatively low to high values among the five canals. For example, the sites of C-11 canal had relatively high A_{AGR}/A_{BUL}, TP/TP_0, TN/TN_0, and Chl a/Chl a_0, while demonstrating low L_c/D_c, Sal/Sal_0, GWD/L_c, and DO/DO_{sat} across the wet and dry seasons (corroborated by Table S2). In contrast, most sites of C-13 canal appeared to have higher (than other sites) GWD/L_c and DO/DO_{sat}, as well as lower A_{AGR}/A_{BUL}, TP/TP_0, and Chl a/Chl a_0. However, the Hillsboro canal sites together represented low to high values of different response and predictor pi numbers across the two seasons.

Dominant Dimensionless Numbers and Linkages Based on Optimal Latent Factors

The eigenvalue ≥ 1 criterion led to three independent, latent factors that optimally explained the variance of the data matrices for eight pi numbers for the wet and dry seasons separately (Table 5). Variances explained by the first three factors ranged, respectively, from approximately 38% to 47%, 24% to 27%, and 18% to 22% between the two seasons. Higher loadings of dimensionless numbers on the same factors indicated their stronger linkages. Factor 1 had strong loadings of TN/TN_0 (−0.74 to −0.91), L_c/D_c (0.63 to 0.99), and Sal/Sal_0 (0.76 to 0.97) in both seasons, as well as moderate loadings of Chl a/Chl a_0 (−0.56) and DO/DO_{sat} (0.51) in only the wet season. Factor 2 had notable and strong loadings of A_{AGR}/A_{BUL}, TP/TP_0, and Chl a/Chl a_0 in the wet season (0.77–0.83). However, the TP number loaded moderately on factor 2 (0.57) in the dry season, alongside the moderate loadings of GWD/L_c (−0.56) and the strong loadings of A_{AGR}/A_{BUL} (0.77) and DO/DO_{sat} (−0.95). Factor 3 had high loadings of

Table 5. Major latent factors with the optimized loadings of the pi numbers

Season	Factor	TN/TN_0	TP/TP_0	Chl a/Chl a_0	DO/DO_{sat}	L_c/D_c	GWD/L_c	A_{AGR}/A_{BUL}	Sal/Sal_0
Wet	1	**−0.74**	−0.08	**−0.56**	**0.51**	**0.99**	−0.08	0.17	**0.76**
	2	0.23	**0.77**	**0.83**	−0.14	−0.13	−0.11	**0.79**	0.07
	3	−0.19	0.00	−0.01	**0.78**	−0.05	**0.92**	**−0.50**	0.23
Dry	1	**−0.91**	0.26	0.04	0.30	**0.63**	0.12	0.01	**0.97**
	2	0.18	**0.57**	0.13	**−0.95**	0.12	**−0.56**	**0.77**	−0.12
	3	0.17	**0.53**	**0.99**	−0.05	**−0.64**	0.09	0.18	0.20

Note: Bold values indicate variables having moderate to high loadings on each factor. Factors 1 and 3, respectively, explained the most and least variance in the overall data matrix for each season.

Table 6. PLSR model coefficients (β) of the standardized pi numbers

Response pi numbers	Season	Predictor pi numbers				PLS component	NSE	RSR
		L_c/D_c	GWD/L_c	A_{AGR}/A_{BUL}	Sal/Sal_0			
TN/TN_0	Wet	**−0.43**	−0.06	0.16	**−0.46**	2	0.71	0.52
	Dry	**−0.38**	−0.20	0.03	**−0.64**	2	0.86	0.36
TP/TP_0	Wet	−0.24	0.41	**0.87**	0.05	2	0.57	0.64
	Dry	**−0.51**	0.22	**0.68**	**0.53**	2	0.60	0.61
Chl a/Chl a_0	Wet	**−0.69**	0.28	**0.88**	0.11	2	0.90	0.31
	Dry	**−0.93**	0.09	**0.46**	**0.65**	2	0.83	0.40
DO/DO_{sat}	Wet	0.30	**0.66**	−0.14	0.26	2	0.80	0.43
	Dry	0.07	0.14	**−0.63**	0.32	2	0.68	0.54

Note: NSE = Nash-Sutcliffe efficiency; RSR = ratio of root-mean-square error to the standard deviations of observations. NSE and RSR indicate the goodness-of-fit and accuracy of the model, respectively.

GWD/L_c (0.92) and DO/DO_{sat} (0.78), while a moderate loading of A_{AGR}/A_{BUL} (−0.50) in the wet season. In contrast, the dry season had notable loadings on factor 3 for only TP/TP_0 (0.53), L_c/D_c (−0.64), and Chl a/Chl a_0 (0.99).

Estimated Relative Linkages between the Response and Predictor pi Numbers

A synthesis of the minimum AIC and maximum NSE led to the inclusion of two PLS components for achieving the power-law based optimum PLSR models of the water quality response pi numbers (Fig. S1 in Supplemental Data). Model fitting efficiency (NSE = 0.57–0.90) and accuracy (RSR = 0.31–0.64), as well as the observed versus predicted plots (Fig. S2 in Supplemental Data) indicated an acceptable performance of the optimal models. Since the PLSR models were estimated on the orthogonal domain with a minimum number of independent PLS components, multicollinearity among the predictor dimensionless numbers were optimally resolved. The model coefficients (Table 6), therefore, provided relatively unbiased (compared to the correlation coefficients) and direct estimations (compared to the PCA and FA results) of the individual contributions of different predictor pi numbers to the variance of a response pi number.

TN/TN_0 had notably stronger linkages with L_c/D_c and Sal/Sal_0 than that with GWD/L_c and A_{AGR}/A_{BUL} across the wet and dry seasons (Table 6). The linkages of TN/TN_0 and L_c/D_c were similar ($\beta = -0.38$ to -0.43) between the two seasons. However, the linkage between TN/TN_0 and Sal/Sal_0 was substantially higher in the dry season ($\beta = -0.64$) than that of the wet season ($\beta = -0.46$). In contrast, TP/TP_0 in the wet season had a dictating linkage with the land-use number (A_{AGR}/A_{BUL}; $\beta = 0.87$), compared to that of L_c/D_c, GWD/L_c, and Sal/Sal_0. Although the strongest control of TP/TP_0 in the dry season was also represented by A_{AGR}/A_{BUL} ($\beta = 0.68$), additional notable controls were demonstrated by L_c/D_c ($\beta = -0.51$) and Sal/Sal_0 ($\beta = 0.53$). Similar to TP/TP_0, Chl a/Chl a_0 was most strongly linked with A_{AGR}/A_{BUL} in the wet season. However, unlike TP/TP_0 and alike TN/TN_0, the wet season Chl a/Chl a_0 also had a relatively strong linkage with L_c/D_c ($\beta = -0.69$). In contrast, Chl a/Chl a_0 in the dry season had the highest linkage with L_c/D_c ($\beta = -0.93$), followed by Sal/Sal_0 ($\beta = 0.65$) and A_{AGR}/A_{BUL} ($\beta = 0.46$). Remarkably, the wet season DO/DO_{sat} had a dictating linkage with GWD/L_c ($\beta = 0.66$), emphasizing the predominant role of hyporheic (groundwater-surface water) exchanges. However, the land-use number had a dictating control on DO/DO_{sat} ($\beta = -0.63$) in the dry season, compared to the other three predictor pi numbers.

Discussion

The research leverages the knowledge on major land-use and hydrologic drivers of coastal-urban stream water quality from Abdul-Aziz and Ahmed (2017) to formulate mechanistically meaningful and important dimensionless numbers. Unlike the environmental controls of individual drivers presented in Abdul-Aziz and Ahmed (2017), the formulated dimensionless numbers in the current study indicated the emergent (collective as well as contrasting) controls of stream water quality in coastal-urban streams. Convergence of results from the four layers of data analytics unequivocally suggested hydrologic control number (L_c/D_c) and salinity number (Sal/Sal_0) as the most important driver numbers for stream TN/TN_0 across the wet and dry seasons. In contrast, based on a synthesis incorporating the two seasons, the land-use number (A_{AGR}/A_{BUL}), L_c/D_c, and Sal/Sal_0 represented the most notable and meaningful mechanistic controls on both TP/TP_0 and Chl a/Chla_o. However, stream DO/DO_{sat} was predominantly driven by the hyporheic exchange number (GWD/L_c) in the wet season and by A_{AGR}/A_{BUL} in the dry season. Overall, dimensional analysis and data analytics reduced nine original variables to a set of three to four important and mechanistically meaningful dimensionless numbers (including both predictor and response numbers) for each water quality indicator. This is a remarkable example of ecohydrological-biogeochemical similitudes (parametric reductions) and a new contribution to the watershed-scale study of coastal-urban stream water quality processes. This is particularly useful for small data sets, which are often encountered in stream water quality and ecosystem health problems. The meaningful set of dominant dimensionless numbers can provide important insights and valuable understanding into the underlying controls and dynamics of coastal-urban stream water quality.

The strong negative linkage of TN/TN_0 with L_c/D_c indicated the dominant control of external drivers (influxes from the Everglades; represented by D_c) on in-stream nitrogen, compared to the surface runoff of the draining watersheds (represented by L_c). The external control was corroborated by the weak positive linkage of TN/TN_0 with A_{AGR}/A_{BUL}, suggesting that the draining watershed land uses (AGR = agriculture + vegetation) had not been any major sources of TN in these urban streams. Instead, longer L_c (larger watersheds and increasing L_c/D_c) generated higher runoff from the predominantly built lands (64.5%), leading to dilution of in-stream TN. In contrast, increasing TN/TN_0 with increasing D_c (decreasing L_c/D_c) toward the upstream watersheds suggested the Everglades as the primary source of stream nitrogen (Abdul-Aziz and Ahmed 2017).

Given the resolution of multicollinearity among the predictor numbers (e.g., L_c/D_c versus Sal/Sal_0) with PLSR (Table 6), the strong negative linkage between TN/TN_0 and Sal/Sal_0 emphasized the detrimental impacts of increasing salinity on stream nitrogen near the coast. Salinity adversely affects the metabolism of a microbial community (Jackson and Vallaire 2009)—reducing mineralization of insoluble organic nitrogen settled at the stream-bed and hindering their influx from the benthic zone to the water column (Rietz and Haynes 2003; Jackson and Vallaire 2009). Further, fixation of atmospheric nitrogen and its transfer into surface water (Brock 2001; Gardner et al. 2006) can be negatively impacted with increased salinity (Herbst 1998; Palma et al. 2013) toward the coast.

The strong positive linkage of TP/TP_0 with A_{AGR}/A_{BUL} indicated the predominant control of agricultural and vegetated lands of the draining watersheds on in-stream phosphorus, compared to that of the built lands. The agricultural and vegetated lands, despite being a small fraction (~10%) of the watersheds, were the primary sources of stream TP across the wet and dry seasons due to washoff of fertilizers and dead organic matters by rainfall runoff (Li et al. 2009; Bu et al. 2014; Wan et al. 2014a, b). In contrast, the highly built land uses (~64.5%) of the watersheds contributed to the dilution of in-stream TP by generating a higher surface runoff. Termination of direct sewage discharge into the canals from the regional wastewater treatment plants since 1989 (BCDPEP 2001) also supported dilution, rather than contribution, of in-stream TP by the draining urban watersheds. The internal watershed control on stream phosphorus was further corroborated by the weaker negative linkages of TP/TP_0 and L_c/D_c (than that of A_{AGR}/A_{BUL})—underlining that the Everglades (indicated by a higher D_c) had been a minor source of phosphorus for the urban streams in southeast Florida (Rudnick et al. 1999; Abdul-Aziz and Ahmed 2017). Instead, higher L_c/D_c represented a longer flow path (L_c), leading to a higher loss of phosphorus (e.g., through deposition, sorption, infiltration, and uptake by biotic community; see McDowell et al. 2004) during the watershed transport before reaching the stream, notably in the dry season (Table 6). This is consistent with Gburek et al. (2000) that reported a 50% decrease in phosphorus concentration from headwater to the watershed outlet in the Susquehanna River Basin, in the eastern part of the United States.

The notable positive linkage of TP/TP_0 with Sal/Sal_0 in only the dry season may be attributed to the substantially higher salinity number in the dry season (average $Sal/Sal_0 = 121$) than that of the wet season (average $Sal/Sal_0 = 13$) (Table 3). Salinity decreases the sorption capacity of sediments that binds phosphorus (Fox et al. 1986; Sundareshwar and Morris 1999; Jordan et al. 2008). Therefore, phosphorus is released in the water column through desorption from sediments in highly saline water. Zhang and Huang (2011) previously reported a substantial release of sediment phosphorus in the highly saline water of Florida Bay. Our study suggests that the sediment release of phosphorus is also prevalent in the urban streams of southeast Florida when the in-stream salinity increases substantially in the dry season (Table 1), with the exception of C-11, which had a very low salinity across the two seasons (Table S1).

The similar linkages of Chl $a/\text{Chl}a_o$ and TP/TP_0 with the predictor dimensionless numbers reiterated TP as the limiting nutrient in the managed urban canals of southeast Florida. This is consistent with the previous studies that reported phosphorus limitation in south Florida's bays and estuaries (e.g., Briceño et al. 2013), Everglades (Noe et al. 2001; Childers et al. 2006), and coral reefs off the coast (Lapointe and Bedford 2010). The moderate to strong positive linkages of Chl $a/\text{Chl}a_o$ with A_{AGR}/A_{BUL} can be attributed to the dominant effects of fertilizers (TP) and dead organic matters inputs to the streams from the agricultural and vegetated lands over the dilution effects of built lands by rainfall runoff (Corkum 1996; Li et al. 2009; Bu et al. 2014; Wan et al. 2014a, b). The strong negative linkages of Chl $a/\text{Chl}a_o$ with L_c/D_c can be attributed to the increased phytoplankton biomass with higher concentrations of stream TN toward the upstream (increasing D_c, decreasing L_c/D_c), contributed by runoff from the Everglades (Brand 2002; NRC 2002). Conversely, higher dilution of stream nitrogen and/or loss of phosphorus during watershed transport by, respectively, higher runoff and/or longer flow path for larger watersheds (higher L_c, increasing L_c/D_c) might have contributed to a decrease in stream biomass. However, the stronger negative linkage of Chl $a/\text{Chl}a_o$ and L_c/D_c in the dry season (than in the wet season) emphasized the impact of basin deposition, adsorption, and infiltration (than dilution) of the limiting nutrient (TP) on stream biomass during transport through a longer flow path. Further, the strong positive linkage of Chl $a/\text{Chl}\,a_0$ with Sal/Sal_0 in only the dry season can be attributed to the sediment release of dissolved inorganic phosphorus due to the higher salinity (Sundareshwar and Morris 1999; Jordan et al. 2008) during low freshwater flow in the canals.

The dictating linkage of DO/DO_{sat} with GWD/L_c in the wet season (Table 6) suggested the predominant control of groundwater-surface water interaction on stream DO due to a higher aquifer recharge and an elevated groundwater table in the study region (Lietz 1999). The strong positive linkage—i.e., higher DO/DO_{sat} with higher GWD/L_c due to a higher groundwater depth from the land surface and a lower hyporheic exchange; and vice versa—may be attributed to the low DO of the underlying, highly transmissive Biscayne aquifer (median = 0.15 mg/L) (Bradner et al. 2005). However, the linkage of DO/DO_{sat} with GWD/L_c was weak in the dry season due to a higher GWD (Tables 1 and S1) and lower hyporheic exchange than that of the wet season. Instead, the dominant and strong negative linkage of DO/DO_{sat} with A_{AGR}/A_{BUL} in the dry season indicated the deteriorating effects of incoming watershed nutrients (specifically, TP) and organic matters (e.g., litters) from the agricultural and vegetated lands during low flow in the canals. The negative linkage further indicated a secondary role of dilution (and/or loss during watershed transport) of nutrients to increase stream DO by higher runoff generation from the predominantly built lands, compared to the adverse impacts of the agricultural and vegetated lands.

Conclusions

The emergent (contrasting as well as collective) controls of coastal-urban stream water quality were evaluated by using similitude and dimensional analysis, considering southeast Florida a prototype of growing coastal-urban environments. Numerous sets of dimensionless pi numbers were derived by changing the repeating variables for four water quality indicators (TN, TP, Chl a, and DO); however, only the mechanistically meaningful sets were chosen for interpretations. The response dimensionless numbers of TN/TN_0, TP/TP_0, and Chl $a/\text{Chl}\,a_0$ represented, respectively, the concentrations of in-stream TN, TP, and Chl a normalized by their immediate upstream reach concentrations. The dimensionless DO/DO_{sat} number was obtained by normalizing the in-stream DO with its saturated concentration (DO_{sat}) to avoid a misleading scaling by the upstream reach concentration in the presence of a DO sag phenomenon. The meaningful predictor numbers included the hydrologic control number (ratio of watershed characteristic length to the distance from coast or proximity to the Everglades), hyporheic exchange number (ratio of groundwater depth from

land surface to watershed characteristic length), land-use number (ratio of agricultural plus vegetated lands to built-up lands), and salinity number (ratio of downstream to upstream salinity). The four predictor numbers represented the collective as well as contrasting controls of land use, hydrologic, and external (e.g., Everglades) drivers on coastal-urban stream water quality in southeast Florida with an acceptable model fitting efficiency and accuracy (NSE = 0.57–0.90; RSR = 0.31–0.64).

The research evaluated the hypothesis that coastal-urban stream water quality processes represent emergent ecohydrological-biogeochemical similitude (parametric reductions). For each of the four water quality indicators, similitude and dimensional analysis reduced nine original variables (including predictors and response) into five mechanistically meaningful dimensionless numbers, which were further reduced to three to four important dimensionless numbers through data analytics. The hydrologic control number and salinity number represented the key controls on stream TN/TN_0 across the wet and dry seasons. The Everglades appeared as the dominant (external) source of in-stream nitrogen, which was diluted by surface runoff from the predominantly built lands (64.5%) of the draining watersheds and was reduced by increasing salinity toward the coast. In contrast, the land-use number, hydrologic control number, and salinity number dominated both TP/TP_0 and $\text{Chl}\,a/\text{Chl}\,a_0$ incorporating the two seasons—reiterating the limiting nutrient in the urban canals of southeast Florida. The agricultural and vegetated lands, despite being a small fraction (~10%) of the draining watersheds, were the main sources of stream phosphorus across the two seasons. Further, the sediment release of dissolved inorganic phosphorus appeared to have augmented stream TP in the dry season due to a higher salinity during the low freshwater flows. However, DO/DO_{sat} was dominated by the hyporheic exchange number in the wet season due to an elevated groundwater table, and by the land-use number in the dry season due to the incoming watershed nutrients (i.e., TP) and organic matters (e.g., litters) from the agricultural and vegetated lands.

The knowledge and insights from the water quality numbers and their dominant predictor numbers are expected to guide water resources management to achieve and/or maintain healthy coastal-urban stream ecosystems, as mandated by the Clean Water Act (FWPCA 2002). The dimensionless numbers can guide water managers to identify streams that are more vulnerable to pollution (than others), and set a priority in management. For example, based on the hydrologic control number, if the stream locations of two watersheds are a similar river-distance away from the Everglades, then the smaller watershed's outlet would have a higher in-stream nitrogen due to less dilution by a lower rainfall runoff. In contrast, the longer flow path of a larger watershed leads to a higher loss of phosphorus during transport through runoff before reaching the stream, notably in the dry season. Therefore, watershed outlets (stream locations) with a lower hydrologic control number would have the higher in-stream nutrients and risk for algal bloom (e.g., Chl *a*). However, given that nitrogen in the urban streams is mainly contributed by the external Everglades, the nitrogen loads should be mitigated in the water conservation areas of the Everglades (Abdul-Aziz and Ahmed 2017). In contrast, the major reduction of stream TP and organic matters would have to be achieved internally by treating runoff from agricultural and vegetated lands of the draining watersheds through detention ponds, for example. Reduction of salinity with control structures during low freshwater flows (especially in the dry season) may further reduce the in-stream phosphorus. Availability of less nutrients is expected to control algal biomass and organic matter, and enhance DO in the streams of southeast Florida and other coastal-urban environments.

Acknowledgments

The research was funded by a CAREER Award to Dr. Omar I. Abdul-Aziz from the US National Science Foundation (NSF CBET Environmental Sustainability Award Number 1561942/1454435). We thank Mr. Robert Bernhard of Broward County, Florida, for sharing an initial study area map and reports with us.

Notation

The following symbols are used in this paper:

A_{AGR} = area of agricultural land (km^2);
A_{BUL} = area of built-up land (km^2);
a, b = exponents of the power-law Eqs. (3) and (4);
$Chla$ = chlorophyll *a* in the stream monitoring station at the subbasin outlet ($\mu g/L$);
$Chla_0$ = chlorophyll *a* in the stream monitoring station at the subbasin inlet ($\mu g/L$);
c, d, e, g = exponents of the power-law Eq. (11);
D_c = stream centerline distance of a water quality monitoring station from the coastline (km);
DO = dissolved oxygen in the stream monitoring station at the subbasin outlet (mg/L);
DO_0 = dissolved oxygen in the stream monitoring station at the subbasin inlet (mg/L);
DO_{sat} = saturated concentration of dissolved oxygen in a stream monitoring station (mg/L);
f = function;
GWD = groundwater depth from the land surface (km);
k = coefficient of a power-law equation;
L = dimension of length;
L_c = subbasin characteristics length (km);
M = dimension of mass;
Sal = salinity in the stream monitoring station at the subbasin outlet (mg/L);
Sal_0 = salinity in the stream monitoring station at the subbasin inlet (mg/L);
TN = total nitrogen in the stream monitoring station at the subbasin outlet (mg/L);
TN_0 = total nitrogen in the stream monitoring station at the subbasin inlet (mg/L);
TP = total phosphorus in the stream monitoring station at the subbasin outlet (mg/L);
TP_0 = total phosphorus in the stream monitoring station at the subbasin inlet (mg/L);
Π_i = dimensionless pi numbers ($i = 1, 2, 3, 4, 5, 6$, and 7); and
ϕ = function.

Supplemental Data

Tables S1–S5, Figs. S1 and S2, and Appendix S1 are available online in the ASCE Library (www.ascelibrary.org).

References

Abdul-Aziz, O. I., and S. Ahmed. 2017. "Relative linkages of stream water quality and environmental health with the land use and hydrologic drivers in the coastal-urban watersheds of southeast Florida." *GeoHealth* 1 (4): 180–195. https://doi.org/10.1002/2017GH000058.

Akaike, H. 1974. "A new look at the statistical model identification." *IEEE Trans. Autom. Control* 19 (6): 716–723. https://doi.org/10.1109/TAC.1974.1100705.

Badruzzaman, M., J. Pinzon, J. Oppenheimer, and J. G. Jacangelo. 2012. "Sources of nutrients impacting surface waters in Florida: A review." *J. Environ. Manage.* 109: 80–92. https://doi.org/10.1016/j.jenvman.2012.04.040.

BCDPEP (Broward County Development of Planning and Environmental Protection). 2001. "Broward County, Florida historical water quality atlas: 1972–1997." Technical Rep. Series TR: 01-03. Accessed March 31, 2015. https://www.broward.org/EnvironmentAndGrowth/EnvironmentalProgramsResources/Publications/Documents/HistWaterQualAtlas72-97.pdf.

BCEPCRD (Broward County Environmental Planning and Community Resilience Division). 2015. "Broward County's ambient water quality program." Accessed March 31, 2015. http://www.broward.org/NaturalResources/Lab/Pages/canalwaterquality.aspx.

BCEPD (Broward County Environmental Protection Department). 2007. *Broward County Florida water quality atlas: Freshwater Canals 1998–2003*. Technical Rep. Series TR: 07-03. Plantation, FL: BCEPD.

Bradner, A., B. F. McPherson, R. L. Miller, G. Kish, and B. Bernard. 2005. *Quality of ground water in the Biscayne aquifer in Miami-Dade, Broward, and Palm Beach Counties, Florida, 1996–1998, with emphasis on contaminants*. Open File Rep. No. 2004-1438. Reston, VA: US Geological Survey.

Brand, L. E. 2002. "The transport of terrestrial nutrients to South Florida coastal waters." In *Proc., The Everglades, Florida Bay and Coral Reefs of the Florida Keys: An Ecosystem Sourcebook*, edited by J. W. Porter and K. G. Porter, 361–414. Washington, DC: CRC Press.

Briceño, H. O., J. N. Boyer, J. Castro, and P. Harlem. 2013. "Biogeochemical classification of South Florida's estuarine and coastal waters." *Mar. Pollut. Bull.* 75 (1): 187–204. https://doi.org/10.1016/j.marpolbul.2013.07.034.

Brock, D. A. 2001. "Nitrogen budget for low and high freshwater inflows, Nueces Estuary, Texas." *Estuaries* 24 (4): 509–521. https://doi.org/10.2307/1353253.

Broward County. 2016. "Environmental assessment team." Accessed April 4, 2016. http://www.broward.org/NaturalResources/Lab/AboutUs/Pages/EnvironmentalAssessmentTeam.aspx.

Bu, H., W. Meng, Y. Zhang, and J. Wan. 2014. "Relationships between land use patterns and water quality in the Taizi River basin, China." *Ecol. Indic.* 41: 187–197. https://doi.org/10.1016/j.ecolind.2014.02.003.

Caccia, V. G., and J. N. Boyer. 2005. "Spatial patterning of water quality in Biscayne Bay, Florida as a function of land use and water management." *Mar. Pollut. Bull.* 50 (11): 1416–1429. https://doi.org/10.1016/j.marpolbul.2005.08.002.

Carey, R. O., K. W. Migliaccio, and M. T. Brown. 2011a. "Nutrient discharges to Biscayne Bay, Florida: Trends, loads, and a pollutant index." *Sci. Total Environ.* 409 (3): 530–539. https://doi.org/10.1016/j.scitotenv.2010.10.029.

Carey, R. O., K. W. Migliaccio, Y. Li, B. Schaffer, A. K. Gregory, and M. T. Brown. 2011b. "Land use disturbance indicators and water quality variability in the Biscayne Bay watershed, Florida." *Ecol. Indic.* 11 (5): 1093–1104. https://doi.org/10.1016/j.ecolind.2010.12.009.

Chang, H. 2008. "Spatial analysis of water quality trends in the Han River basin, South Korea." *Water Res.* 42 (13): 3285–3304. https://doi.org/10.1016/j.watres.2008.04.006.

Chapra, S. C. 2008. *Surface water-quality modeling*. Long Grove, IL: Waveland Press.

Childers, D. L., J. N. Boyer, S. E. Davis, C. J. Madden, D. T. Rudnick, and F. H. Sklar. 2006. "Relating precipitation and water management to nutrient concentrations in the oligotrophic "upside-down" estuaries of the Florida Everglades." *Limnol. Oceanogr.* 51 (1): 602–616. https://doi.org/10.4319/lo.2006.51.1_part_2.0602.

Childs, C. 2004. "Interpolating surfaces in ArcGIS spatial analyst." *ArcUser* 3235: 32–35.

Cooper, R. M., and J. Lane. 1987. *An atlas of Eastern Broward County surface water management basins*. Technical Memorandum, DRE 231. West Palm Beach, FL: South Florida Water Management District.

Corkum, L. D. 1996. "Responses of chlorophyll-a, organic matter, and macroinvertebrates to nutrient additions in rivers flowing through agricultural and forested land." *Arch. Hydrobiol.* 136 (3): 391–411.

Costelloe, J. F., T. J. Peterson, K. Halbert, A. W. Western, and J. J. McDonnell. 2015. "Groundwater surface mapping informs sources of catchment baseflow." *Hydrol. Earth Syst. Sci.* 19 (4): 1599–1613. https://doi.org/10.5194/hess-19-1599-2015.

Daniel, F. B., M. B. Griffith, and M. E. Troyer. 2010. "Influences of spatial scale and soil permeability on relationships between land cover and baseflow stream nutrient concentrations." *Environ. Manage.* 45 (2): 336–350. https://doi.org/10.1007/s00267-009-9401-x.

de Jong, S. 1993. "SIMPLS: An alternative approach to partial least squares regression." *Chemom. Intell. Lab. Syst.* 18 (3): 251–263. https://doi.org/10.1016/0169-7439(93)85002-X.

FDEP (Florida Department of Environmental Protection). 2016. "Florida department of environmental protection geospatial open data." Accessed October 10, 2016. http://geodata.dep.state.fl.us/datasets/d3bb23dc9507422a86c95eb5efc964c9_0.

Finnemore, E. J., and J. B. Franzini. 2002. *Fluid mechanics with engineering applications*. 10th ed. New York: McGraw-Hill.

Fox, L. E., S. L. Sager, and S. C. Wofsy. 1986. "The chemical control of soluble phosphorus in the Amazon estuary." *Geochim. Cosmochim. Acta* 50 (5): 783–794. https://doi.org/10.1016/0016-7037(86)90354-6.

FWPCA (Federal Water Pollution Control Act). 2002. *Federal water pollution control act, as amended through P.L. 107–303, November 27, 2002*. Washington, DC: US Government.

Gardner, W. S., M. J. McCarthy, S. An, D. Sobolev, K. S. Sell, and D. Brock. 2006. "Nitrogen fixation and dissimilatory nitrate reduction to ammonium (DNRA) support nitrogen dynamics in Texas estuaries." *Limnol. Oceanogr.* 51 (1 part 2): 558–568. https://doi.org/10.4319/lo.2006.51.1_part_2.0558.

Gburek, W. J., A. N. Sharpley, L. Heathwaite, and G. J. Folmar. 2000. "Phosphorus management at the watershed scale: A modification of the phosphorus index." *J. Environ. Qual.* 29 (1): 130–144. https://doi.org/10.2134/jeq2000.00472425002900010017x.

Goovaerts, P. 1997. *Geostatistics for natural resources evaluation*. 1st ed. New York: Oxford University Press.

Guentzel, K. S., M. Hondzo, B. D. Badgley, J. C. Finlay, M. J. Sadowsky, and J. L. Kozarek. 2014. "Measurement and modeling of denitrification in sand-bed streams under various land uses." *J. Environ. Qual.* 43 (3): 1013–1023. https://doi.org/10.2134/jeq2013.06.0249.

Hart, B. T., P. Bailey, R. Edwards, K. Hortle, K. James, A. McMahon, C. Meredith, and K. Swadling. 1991. "A review of the salt sensitivity of the Australian freshwater biota." *Hydrobiologia* 210 (1–2): 105–144. https://doi.org/10.1007/BF00014327.

Herbst, D. B. 1998. "Potential salinity limitations on nitrogen fixation in sediments from Mono Lake, California." *Int. J. Salt Lake Res.* 7 (3): 261–274. https://doi.org/10.1007/BF02441878.

Hubert, M., and K. V. Branden. 2003. "Robust methods for partial least squares regression." *J. Chemom.* 17 (10): 537–549. https://doi.org/10.1002/cem.822.

Jackson, C. R., and S. C. Vallaire. 2009. "Effects of salinity and nutrients on microbial assemblages in Louisiana wetland sediments." *Wetlands* 29 (1): 277–287. https://doi.org/10.1672/08-86.1.

Jolliffe, I. T. 2002. *Principal component analysis*. 2nd ed. New York: Springer.

Jordan, T. E., J. C. Cornwell, W. R. Boynton, and J. T. Anderson. 2008. "Changes in phosphorus biogeochemistry along an estuarine salinity gradient: The iron conveyer belt." *Limnol. Oceanogr.* 53 (1): 172–184. https://doi.org/10.4319/lo.2008.53.1.0172.

Kang, J. H., S. W. Lee, K. H. Cho, S. J. Ki, S. M. Cha, and J. H. Kim. 2010. "Linking land-use type and stream water quality using spatial data of fecal indicator bacteria and heavy metals in the Yeongsan river basin." *Water Res.* 44 (14): 4143–4157. https://doi.org/10.1016/j.watres.2010.05.009.

Kuhn, M., and K. Johnson. 2013. *Applied predictive modeling*. New York: Springer.

Kundu, P. K., and I. M. Cohen. 2002. *Fluid mechanics*. 2nd ed. Berkeley, CA: Elsevier Academic Press.

Kundu, P. K., and I. M. Cohen. 2004. *Fluid mechanics*. 3rd ed. New York: Elsevier Academic Press.
Lapointe, B. E., and B. J. Bedford. 2010. "Ecology and nutrition of invasive Caulerpa brachypus f. parvifolia blooms on coral reefs off southeast Florida, USA." *Harmful Algae* 9 (1): 1–12. https://doi.org/10.1016/j.hal.2009.06.001.
Li, S., S. Gu, X. Tan, and Q. Zhang. 2009. "Water quality in the upper Han River basin, China: The impacts of land use/land cover in riparian buffer zone." *J. Hazard. Mater.* 165 (1–3): 317–324. https://doi.org/10.1016/j.jhazmat.2008.09.123.
Lietz, A. C. 1999. *Methodology for estimating nutrient loads discharged from the east coast canals to Biscayne Bay, Miami-Dade County, Florida*. Water-Resources Investigations Rep. No. 99-4094. Tallahassee, FL: US Geological Survey.
Liu, D., X. Chen, and Z. Lou. 2010. "A model for the optimal allocation of water resources in a saltwater intrusion area: A case study in Pearl River delta in China." *Water Resour. Manage.* 24 (1): 63–81. https://doi.org/10.1007/s11269-009-9437-y.
Magalhães, C. M., S. B. Joye, R. M. Moreira, W. J. Wiebe, and A. A. Bordalo. 2005. "Effect of salinity and inorganic nitrogen concentrations on nitrification and denitrification rates in intertidal sediments and rocky biofilms of the Douro River estuary, Portugal." *Water Res.* 39 (9): 1783–1794. https://doi.org/10.1016/j.watres.2005.03.008.
McDowell, R. W., B. J. F. Biggs, A. N. Sharpley, and L. Nguyen. 2004. "Connecting phosphorus loss from agricultural landscapes to surface water quality." *Chem. Ecol.* 20 (1): 1–40. https://doi.org/10.1080/02757540310001626092.
Menció, A., and J. Mas-Pla. 2008. "Assessment by multivariate analysis of groundwater-surface water interactions in urbanized Mediterranean streams." *J. Hydrol.* 352 (3): 355–366. https://doi.org/10.1016/j.jhydrol.2008.01.014.
Miragliotta, G. 2011. "The power of dimensional analysis in production systems design." *Int. J. Prod. Econ.* 131 (1): 175–182. https://doi.org/10.1016/j.ijpe.2010.08.009.
Morris, M. W., and M. Hondzo. 2013. "Glossosoma nigrior (Trichoptera: Glossosomatidae) respiration in moving fluid." *J. Exp. Biol.* 216 (16): 3015–3022. https://doi.org/10.1242/jeb.082974.
Nash, J. E., and J. V. Sutcliffe. 1970. "River flow forecasting through conceptual models. Part I: A discussion of principles." *J. Hydrol.* 10 (3): 282–290. https://doi.org/10.1016/0022-1694(70)90255-6.
Noe, G. B., D. L. Childers, and R. D. Jones. 2001. "Phosphorus biogeochemistry and the impact of phosphorus enrichment: Why is the Everglades so unique?" *Ecosystems* 4 (7): 603–624. https://doi.org/10.1007/s10021-001-0032-1.
NRC (National Research Council). 2002. *Florida Bay research programs and their relation to the comprehensive Everglades restoration plan*. Washington, DC: National Academies Press.
NSRDB (National Solar Radiation Data Base). 2017. "NSRDB data viewer." Accessed January 15, 2017. https://maps.nrel.gov/nsrdb-viewer/.
NWQMC (National Water Quality Monitoring Council). 2017. "Water quality data." Accessed January 10, 2017. https://www.waterqualitydata.us/portal/.
Palma, F., M. López-Gómez, N. A. Tejera, and C. Lluch. 2013. "Salicylic acid improves the salinity tolerance of Medicago sativa in symbiosis with *Sinorhizobium meliloti* by preventing nitrogen fixation inhibition." *Plant Sci.* 208: 75–82. https://doi.org/10.1016/j.plantsci.2013.03.015.
Rietz, D. N., and R. J. Haynes. 2003. "Effects of irrigation-induced salinity and sodicity on soil microbial activity." *Soil Biol. Biochem.* 35 (6): 845–854. https://doi.org/10.1016/S0038-0717(03)00125-1.
Rudnick, D. T., Z. Chen, D. L. Childers, and T. D. Fontaine. 1999. "Phosphorus and nitrogen inputs to Florida Bay: The importance of the Everglades watershed." *Estuaries* 22 (2): 398–416. https://doi.org/10.2307/1353207.
Schumann, S., L. P. Nolte, and G. Zheng. 2013. "Comparison of partial least squares regression and principal component regression for pelvic shape prediction." *J. Biomech.* 46 (1): 197–199. https://doi.org/10.1016/j.jbiomech.2012.11.005.
SFWMD (South Florida Water Management District). 2015a. "Land cover land use." Accessed March 2, 2015. http://sfwmd.maps.arcgis.com/home/item.html?id=989eb66b1b3b43fc9ddd30d29eaf0904.
SFWMD (South Florida Water Management District). 2015b. "The current weather conditions: Florida radar loop." Accessed March 1, 2015. http://www.sfwmd.gov/portal/page/portal/levelthree/weather%20%20water.
SFWMD (South Florida Water Management District). 2016. "DBHYDRO." Accessed April 11, 2016. http://my.sfwmd.gov/dbhydroplsql/show_dbkey_info.show_dbkeys_matched?v_station=WCA2F4.
Sprague, L. A. 2005. "Drought effects on water quality in the South Platte River Basin, Colorado." *J. Am. Water Resour. Assoc.* 41 (1): 11–24. https://doi.org/10.1111/j.1752-1688.2005.tb03713.x.
Sundareshwar, P. V., and J. T. Morris. 1999. "Phosphorus sorption characteristics of intertidal marsh sediments along an estuarine salinity gradient." *Limnol. Oceanogr.* 44 (7): 1693–1701. https://doi.org/10.4319/lo.1999.44.7.1693.
Tran, C. P., R. W. Bode, A. J. Smith, and G. S. Kleppel. 2010. "Land-use proximity as a basis for assessing stream water quality in New York State (USA)." *Ecol. Indic.* 10 (3): 727–733. https://doi.org/10.1016/j.ecolind.2009.12.002.
Tufford, D. L., C. L. Samarghitan, H. N. McKellar, D. E. Porter, and J. R. Hussey. 2003. "Impacts of urbanization on nutrient concentrations in small southeastern coastal streams." *J. Am. Water Resour. Assoc.* 39 (2): 301–312. https://doi.org/10.1111/j.1752-1688.2003.tb04385.x.
USGS. 2015a. "A TNM download." Accessed March 1, 2015. https://viewer.nationalmap.gov/basic/.
USGS. 2015b. "National water information system: Mapper." Accessed April 22, 2015. https://maps.waterdata.usgs.gov/mapper/index.html.
Wan, R., S. Cai, H. Li, G. Yang, Z. Li, and X. Nie. 2014a. "Inferring land use and land cover impact on stream water quality using a Bayesian hierarchical modeling approach in the Xitiaoxi River watershed, China." *J. Environ. Manage.* 133: 1–11. https://doi.org/10.1016/j.jenvman.2013.11.035.
Wan, Y., Y. Qian, K. W. Migliaccio, Y. Li, and C. Conrad. 2014b. "Linking spatial variations in water quality with water and land management using multivariate techniques." *J. Environ. Qual.* 43 (2): 599–610. https://doi.org/10.2134/jeq2013.09.0355.
Warnaars, T. A., M. Hondzo, and M. E. Power. 2007. "Abiotic controls on periphyton accrual and metabolism in streams: Scaling by dimensionless numbers." *Water Resour. Res.* 43 (8): W08425. https://doi.org/10.1029/2006WR005002.
Wold, S., M. Sjöström, and L. Eriksson. 2001. "PLS-regression: A basic tool of chemometrics." *Chemom. Intell. Lab. Syst.* 58 (2): 109–130. https://doi.org/10.1016/S0169-7439(01)00155-1.
Woodcock, T., T. Mihuc, E. Romanowicz, and E. Allen. 2006. "Land-use effects on catchment-and patch-scale habitat and macroinvertebrate responses in the Adirondack uplands." In Vol. 84 of *Proc., Symp. on Influence of Landscape on Stream Habitat and Biological Communities*, edited by R. M. Hughes, L. Wang, and P. W. Seelbach, 395–411. Bethesda, MD: American Fisheries Society.
Xiao, R., G. Wang, Q. Zhang, and Z. Zhang. 2016. "Multi-scale analysis of relationship between landscape pattern and urban river water quality in different seasons." *Sci. Rep.* 6 (1): 25250. https://doi.org/10.1038/srep25250.
Xie, R., Y. Pang, B. Luo, J. Li, C. Wu, Y. Zheng, Q. Sun, P. Zhang, and F. Wang. 2017. "Spatiotemporal variability in salinity and hydraulic relationship with salt intrusion in the tidal reaches of the Minjiang River, Fujian Province, China." *Environ. Sci. Pollut. Res.* 24 (12): 11847–11855. https://doi.org/10.1007/s11356-017-8788-9.
Zeleňáková, M., M. Čarnogurská, M. Šlezingr, D. Słyś, and P. Purcz. 2013. "A model based on dimensional analysis for prediction of nitrogen and phosphorus concentrations at the river station Ižkovce, Slovakia." *Hydrol. Earth Syst. Sci.* 17 (1): 201–209. https://doi.org/10.5194/hess-17-201-2013.
Zhang, J. Z., and X. L. Huang. 2011. "Effect of temperature and salinity on phosphate sorption on marine sediments." *Environ. Sci. Technol.* 45 (16): 6831–6837. https://doi.org/10.1021/es200867p.